AFDL Dipole (SwissFEL, Linac Beam Dump)

AFDL (Linac beam dump dipole)
on picture is the beam entrance end

gap = 22 mm

L1000 x W470 x H430 mm
20° (±10°) bend

conductor: 7.5 x 7.5, D 4.5 mm
96 turns/coil, I_{MAX} = 135 A

enameled wire: D 2.5 mm
18 turns/coil, I_{MAX} = 10 A

MEASUREMENT DATE:
9 Jul. – 3 Sep. 2015

MEASUREMENT ARM:
brass cylinder interface Ø 40 mm
aluminum pipe Ø 28 mm, 1 m
carbon pipes Ø 10/8/6 mm, 1.5 m

MEASURING SPEED:
24 mm/sec (Z-axis)

INTEGRATION TIME:
20 msec

DVM-1 (1 V RANGE):
Hall probe sbv175s (150 mA)
powered on its own
AZERO = ON

DVM-2 (10 V RANGE):
40 V / 150 A (ext), 5 A/s
24 V / 10 A (MSG2.3), 1 A/s

AIR CONDITIONING:
ON (T_{SET} = 24.5°)

OPERATORS:
Vjeran Vranković
Roland Deckardt

DATA DIRECTORY:
afs: group/magnet/meas/
SwissFEL/afdl

Overview

PS MAXIMUM CURRENT:
135 A (main coil)
10 A (correction coil)

PS CURRENT RAMP:
5 A/s

PRE-CYCLING:
1 A → 135 A → 1 A → 135 A

FIELD SETTLING TIME:
45 s (10^{-4})

CURRENT SETTING:
I_{OLD} → 135 A → I_{NEW}

DEGAUSSING:
I_{ANY} → 135 A → -27.5 A → OFF

WATER PRESSURE DROP:
4 bar

WATER TEMPERATURE INCREASE:
50 A → 1.2 °C
130 A → 8.6 °C
135 A → 9.2 °C

TIME FOR 99% TEMPERATURE INCREASE:
15 min

BENDING:
bending angle (to the right) 20°
bending radius 2925.5 mm

CONSTANT EFFECTIVE LENGTH:
straight 1016 mm
curved 1021 mm

EXCITATION INITIAL SLOPE:
108.687 Gauss/Amp

STRAIGHT FIELD INTEGRALS:
0.014 – 1.441 Tm (main, 1–135A)
±0.020 Tm (correction, ±10 A)

BEAM-VERTEX TO MAGNET-CENTER:
67–74 mm

FIELD HOMOGENEITY OVER ±5 MM:
vertex: from 67 mm 74 mm
quadrupole: from 278 to 90 ppm
sextupole: from -40 to -100 ppm

CURRENT VS. BEAM ENERGY:
20 A → 0.193 GeV
130 A → 1.213 GeV

Magnet alignment and positioning

The positioning was done by the double reference pin, the famous “Brueno”, inserted into 4 holes on top of the magnet return yoke. The beam entrance magnet end was measured first and then the measuring arm was extended to allow for the measurements of the beam exit magnet end.

Eventually the magnet was remeasured in one go, i.e. both magnet ends were measured in the single field maps.

The electrical connection for the main coil were such that a positive current caused the bottom magnet pole to become the NORTH magnetic pole. The same principle was used for the correction coils - positive current created the NORTH pole at the bottom of the magnet. After the measurements were completed the polarity of the main coil was swapped (M. Negrazus on 3 Sep 2015). The correction coil electrical connections remained the same.

Therefore with the current electrical connections, the positive current in the main coil causes the electron beam to bend to the right (into the beam dump), but the positive current in the correction coil causes the electron beam to bend to the left.

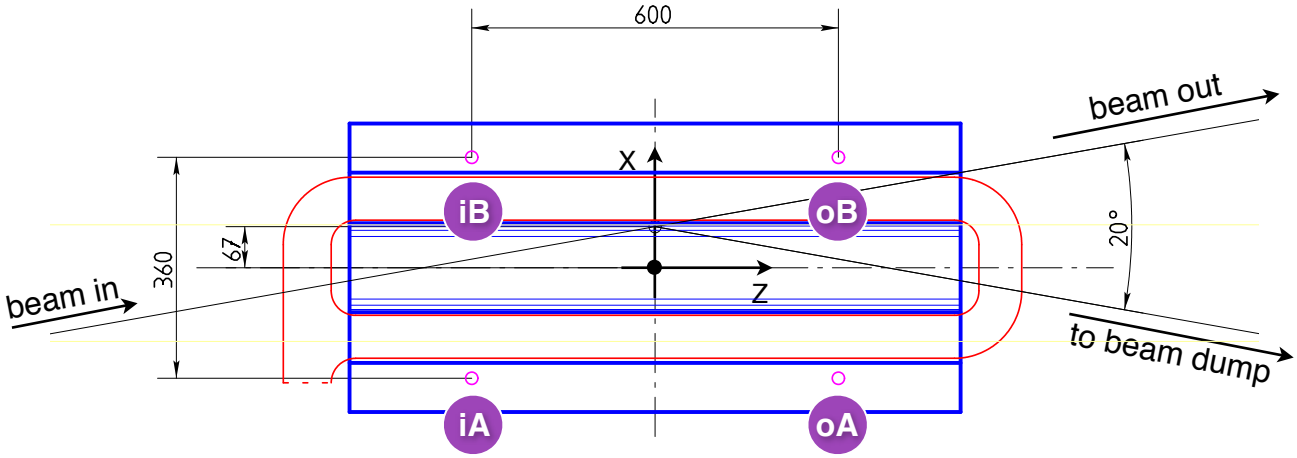

Magnet alignment and positioning

	file	date	Y	Z	X	Bfit	dist i/o	dist A/B
beam entrance	**iA-2**	4 Aug 2015	-0.630	201.350	95.847	-570.76	359.985	600.021
	iB-2	4 Aug 2015	-0.580	201.249	455.832	-570.57		
	oB-1	4 Aug 2015	-0.530	801.345	455.861	-571.18	359.980	600.096
	oA-1	4 Aug 2015	-0.590	801.371	95.881	-570.86		
	average		**-0.583**	**501.329**	**275.855**	**set to Y = 259 mm, Z = X = 0**		
	iA		**258.953**	**-299.979**	**-180.008**			
	iB		259.003	-300.080	179.977			
	oB		259.053	300.016	180.006			
	oA		258.993	300.042	-179.974			
beam exit	**iA-4**	15 Aug 2015	255.540	-485.303	-180.537	-569.83	360.124	600.029
	iB-3	15 Aug 2015	255.600	-485.249	179.587	-569.88		
	oB-2	15 Aug 2015	255.620	114.842	179.617	-570.28	360.128	600.091
	oA-2	15 Aug 2015	255.560	114.726	-180.511	-570.04		
	average		**255.580**	**-185.246**	**-0.461**	**set to Y = 259 mm, Z = X = 0**		
	iA		**258.960**	**-300.057**	**-180.076**			
	iB		259.020	-300.003	180.048			
	oB		259.040	300.088	180.078			
	oA		258.980	299.972	-180.050			
both beam entrance and exit	**iA-5**	20 Aug 2015	260.690	-280.750	-180.007	-569.68	359.996	600.077
	iB-4	20 Aug 2015	260.740	-280.844	179.989	-569.83		
	oB-3	20 Aug 2015	260.760	319.256	180.064	-570.33	360.045	600.100
	oA-3	20 Aug 2015	260.700	319.327	-179.981	-570.15		
	average		**260.723**	**19.247**	**0.016**	**set to Y = 259 mm, Z = X = 0**		
	iA		**258.968**	**-299.997**	**-180.023**			
	iB		259.018	-300.091	179.973			
	oB		259.038	300.009	180.048			
	oA		258.978	300.080	-179.997			

Current ramp setting

The AFDL magnet body is made out of solid iron and is therefore prone to eddy current losses. Different slopes of current ramping will significantly (at the 0.01% level) affect the magnetic field reproducibility.

Effects of 3 different current ramps have been considered and for the time saving reason during the cycling of the magnet, a current ramp of 5 A/s was chosen together with a settling time of at least 30 s after the set current is reached.

NOTE – On few occasions it was observed that the current ramp of the power supply unintentionally changed (see the screenshot for one of these occurrences).

	5 A/s	2 A/s	1 A/s
time to ramp 135 A → 75 A	12 s	30 s	60 s
current overshoot 135 A → 75 A	10 mA	2 mA	0.5 mA
stable field at 75 A (t = ∞)		~8200 Gauss	
field difference at the end of ramp (t = 0)	162 Gauss	84 Gauss	56 Gauss
settling time for 0.1% of B_0	14 s	11 s	7 s
settling time for 0.05% of B_0	22 s	17 s	11 s
settling time for 0.02% of B_0	33 s	27 s	19 s
settling time for 0.01% of B_0	42 s	34 s	25 s

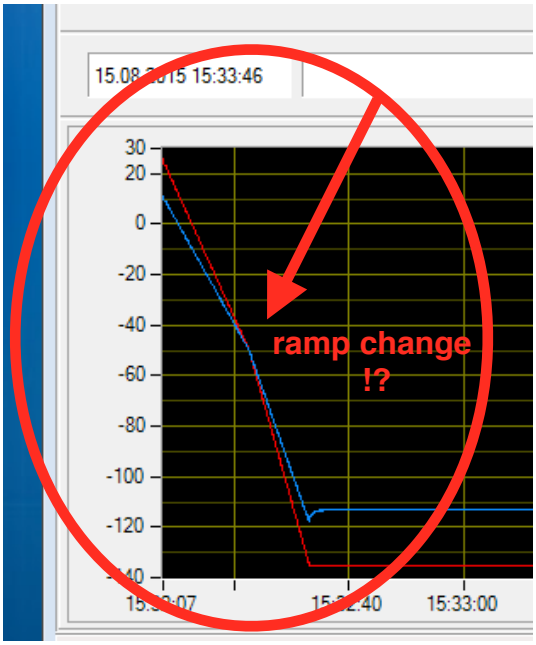

Pre-cycling procedure (-135 A → +135 A)

To determine an accurate pre-cycling procedure the NMR probe was placed in the magnet gap somewhere at the beam exit magnet end, at a position where the magnetic field is homogeneous.

After the first hysteresis loop and coming to the maximum current +135 A for the second time, the field difference is over 18 Gauss or 0.13%. After the second loop it is already less than 0.1 Gauss. Further looping does not significantly increase the field reproducibility which eventually stabilizes around 10 ppm.

measured with NMR Teslameter Metrolab PT2025					
1	**degaussed → +135 A**	14186.04			
	+135 A → -135 A	14204.37			
	-135 A → +135 A	14204.52	18.48	0.1301%	
2	**+135 A → -135 A**	14203.60	-0.77	-0.0054%	
	-135 A → +135 A	14204.47	-0.05	-0.0004%	
3	**+135 A → -135 A**	14203.54	-0.06	-0.0004%	
	-135 A → +135 A	14204.50	0.03	0.0002%	
4	**+135 A → -135 A**	14203.55	0.01	0.0001%	
	-135 A → +135 A	14204.47	-0.03	-0.0002%	
5	**+135 A → -135 A**	14203.30	-0.25	-0.0018%	PS disobeyed the ramp
	-135 A → +135 A	14204.41	-0.06	-0.0004%	
6	**+135 A → -135 A**	14203.49	0.19	0.0013%	
	-135 A → +135 A	14204.31	-0.10	-0.0007%	
1	**off → +135 A**	14184.75			
	+135 A → -135 A	14204.15			
	-135 A → +135 A	14204.42	19.67	0.1385%	
2	**+135 A → -135 A**	14203.47	-0.68	-0.0048%	
	-135 A → +135 A	14204.32	-0.10	-0.0007%	

Pre-cycling procedure (+10 A → +135 A)

Another hysteresis loop was tested, where the magnet cycles around positive currents only. The minimum current was not taken at 0 A because of the unreliable PS behavior at this point, instead 10 A was chosen.

After the first hysteresis loop the field difference at the maximum current +135 A is around 3 Gauss or 0.02%, after the second it is 0.5 Gauss or 30 ppm and then it continually decreases to around 10 ppm.

Although the field reproducibility with cycling around positive currents only is slightly worse than when compared to ±135 A loop, it has been chosen due to its time savings of around 1 min per cycle.

The minimum current has later been set at +1 A.

measured with NMR Teslameter Metrolab PT2025				
	degaussed → 135 A	14185.82		
1	**135 A → 10A → 135 A**	14182.49	-3.33	-0.0235%
2	**135 A → 10A → 135 A**	14182.01	-0.48	-0.0034%
3	**135 A → 10A → 135 A**	14181.80	-0.21	-0.0015%
4	**135 A → 10A → 135 A**	14181.64	-0.16	-0.0011%
5	**135 A → 10A → 135 A**	14181.55	-0.09	-0.0006%
6	**135 A → 10A → 135 A**	14181.48	-0.07	-0.0005%
	off → 135 A	14182.07		
1	**135 A → 10A → 135 A**	14181.43	-0.64	-0.0045%
2	**135 A → 10A → 135 A**	14181.39	-0.04	-0.0003%
3	**135 A → 10A → 135 A**	14181.37	-0.02	-0.0001%
4	**135 A → 10A → 135 A**	14181.33	-0.04	-0.0003%

Precise field setting

The magnet PS overshoots the set current with an amount that depends on the current ramp and on the difference between the start and the end current. This has an effect on the field and although for a given combination the magnetic field is reproducible it is not predictable for any combination.

For instance setting the magnet current to 75 A with the ramp of 5 A/s, in one case directly from 135 A and in the other stopping on the way at every 10 A, results in the field difference of over 8 Gauss or 0.1%. This difference is reduced to 4 Gauss with the ramp of 2 A/s and then further reduced to 2 Gauss with the ramp of 1 A/s.

One can achieve a small enough error with slow current ramps but at the expense of the long setting time. An alternative has been proposed in which the current ramp is kept reasonably fast at 5 A/s but setting to a new current is around the pre-cycling loop:

$I_{OLD} \rightarrow I_{MIN} \rightarrow I_{MAX} \rightarrow I_{NEW}$

In this way the field reproducibility is guaranteed and also known to better than 0.01%.

hysteresis loop -135 A → +135 A; X = 0, Y = 0, Z = -810 : +810 (18–20 August 2015)							
I A	**in out**	**B_2** Gauss/mm	**B·dz** Tm	**B_0** Gauss	**L_{EFF}** mm	**Δ(B·dz)** relative	**ΔB_0** relative
75	I 76	1 x -60 A, 5 A/s	-0.83244	-8194.6	1015.8		
	I 77	2 x -30 A, 5 A/s	-0.83263	-8196.7	1015.8	0.02%	0.03%
	I 78	3 x -20 A, 5 A/s	-0.83286	-8199.1	1015.8	0.05%	0.06%
	I 79	6 x -10 A, 5 A/s	-0.83327	-8203.3	1015.8	0.10%	0.11%
	I 80	1 x -60 A, 5 A/s	-0.83245	-8194.7	1015.8	0.00%	0.00%
	I 81	1 x -60 A, 2 A/s	-0.83318	-8202.4	1015.8		
	I 82	6 x -10 A, 2 A/s	-0.83358	-8206.3	1015.8	0.05%	0.05%
	I 83	1 x -60 A, 1 A/s	-0.83369	-8207.1	1015.8		
	I 84	6 x -10 A, 1 A/s	-0.83385	-8208.9	1015.8	0.02%	0.02%
	I 85	from precyc, 5 A/s	-0.83247	-8194.9	1015.8	0.00%	0.00%
	I 87	I_{OLD} = 120 A, 5 A/s	-0.83248	-8195.0	1015.8	0.00%	0.01%
	I 89	I_{OLD} = 40 A, 5 A/s	-0.83248	-8195.0	1015.9	0.01%	0.00%

Precise field setting

The following table summarizes investigations to the field reproducibility at the maximum current after different changes in the current reverse directions have been applied, the current set to I_{MIN} = 1 A and then to I_{MAX} = 135 A.

x_L: 20 A → 30 A
x_M: 75 A → 85 A
x_H: 120 A → 130 A

All these cases show no effect on the field reproducibility that is higher than 0.01%.

hysteresis loop +1 A → +135 A; X = 0, Y = 0, Z = -840 : +840 (21 August 2015)							
I A	**in out**	**B_2** Gauss/mm	**B·dz** Tm	**B_0** Gauss	**L_{EFF}** mm	**Δ(B·dz)** relative	**ΔB_0** relative
	I 90	off →	-1.44084	-14206.1	1014.2		
	I 91	1 → (1st)	-1.44075	-14205.1	1014.3	-0.006%	-0.007%
	I 92	1 → (2nd)	-1.44075	-14205.0	1014.3	-0.000%	-0.001%
	I 93	1 → (3rd)	-1.44073	-14204.8	1014.3	-0.001%	-0.001%
	I 94	off (demag) →	-1.44087	-14206.1	1014.3	0.010%	0.009%
	I 95	1 → (1st)	-1.44071	-14204.4	1014.3	-0.011%	-0.012%
135	I 96	1 → (2nd)	-1.44071	-14204.4	1014.3	-0.000%	0.000%
	I 97	x_M→1 → (1st)	-1.44075	-14205.0	1014.3	0.003%	0.004%
	I 98	x_M→1 → (2nd)	-1.44070	-14204.3	1014.3	-0.004%	-0.005%
	I 99	x_H→1 → (1st)	-1.44069	-14204.2	1014.3	-0.001%	-0.001%
	I 100	x_H→1 → (2nd)	-1.44068	-14204.1	1014.3	-0.001%	-0.001%
	I 101	x_L→1 → (1st)	-1.44072	-14204.7	1014.3	0.003%	0.004%
	I 102	x_L→1 → (2nd)	-1.44068	-14204.1	1014.3	-0.003%	-0.004%

Degaussing

Degaussing of the magnet is achieved with I_{DG} = -27.5 A. The best demagnetization is achieved by going around the hysteresis loop 1 A → 135 A → -27.5 A → 0, but also demagnetizations from any other current I → -27.5 A → 0 will yield the remnant field integral values below ±0.00005 Tm.

hysteresis loop +1 A → +135 A; X = 0, Y = 0, Z = -840 : +840 (21 August 2015)				
I A	**in** **out**	**B_2** Gauss/mm	**B·dz** Tm	**B_0** Gauss
off	I 103	off → 135 A → 1 A → 135 A → off	-0.00309	-29.6
	I 104	off → -26 A → off	-0.00015	-2.0
	I 105	off → -27.5 A → off	0.00002	-0.3

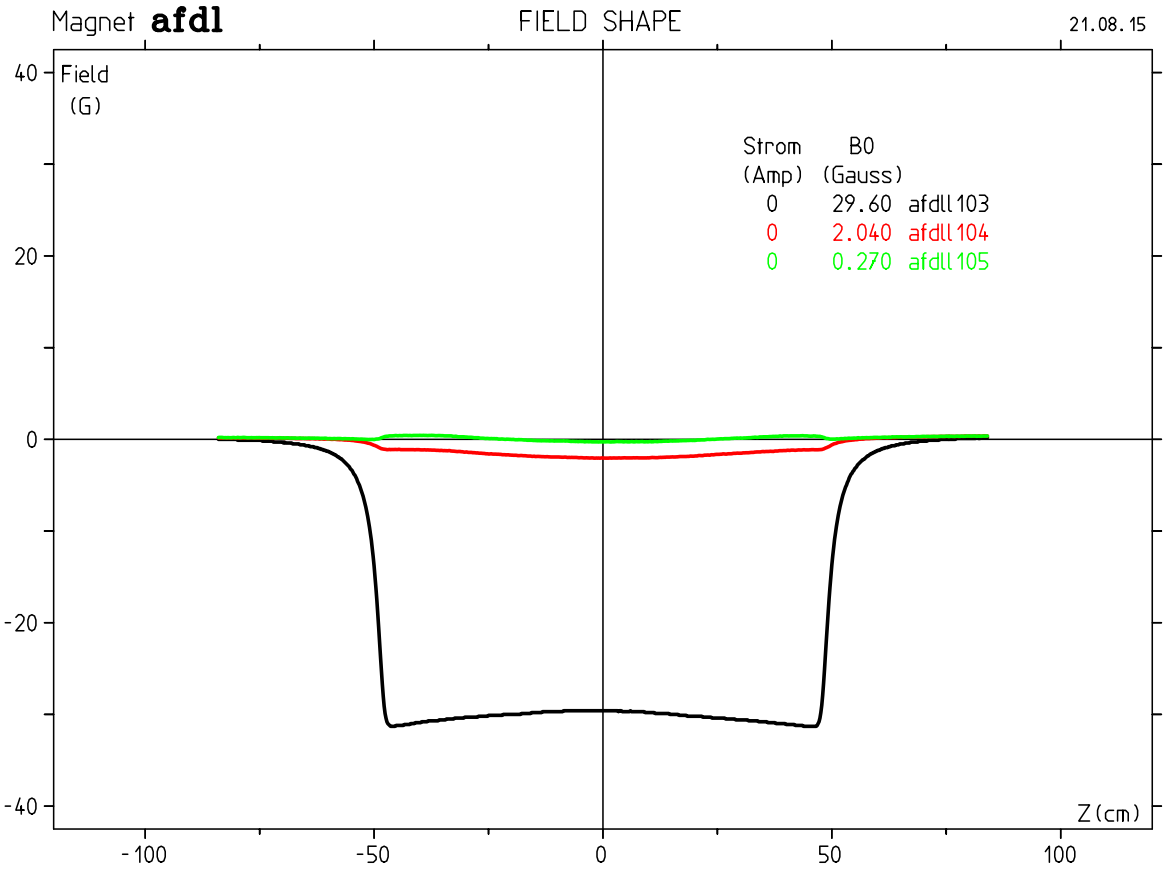

Excitation curve (main coil)

Before measurements the magnet was pre-cycled 2 times around the loop from 1 A to 135 A. The fields were then measured at 39 currents always coming down directly from 135 A to the set current, on the line X = Y = 0, Z = -840 : +840 mm.

The standard linear/cubic fit describes the excitation curve to not better than 0.3%. A much higher relative accuracy of 0.002% is achieved with a cubic spline fit. A lookup table for beam energies versus the magnet current is calculated for all the currents from 2 A to 134 A at every 1 A.

NOTE - The measured field sign has been changed to positive for the easier interpretation against the current. In any case the measured field sign is irrelevant as it is defined by the orientation of the used Hall probe in the magnetic field. For the AFDL measurements the negative measured fields mean that the BOTTOM pole is the NORTH magnetic pole.

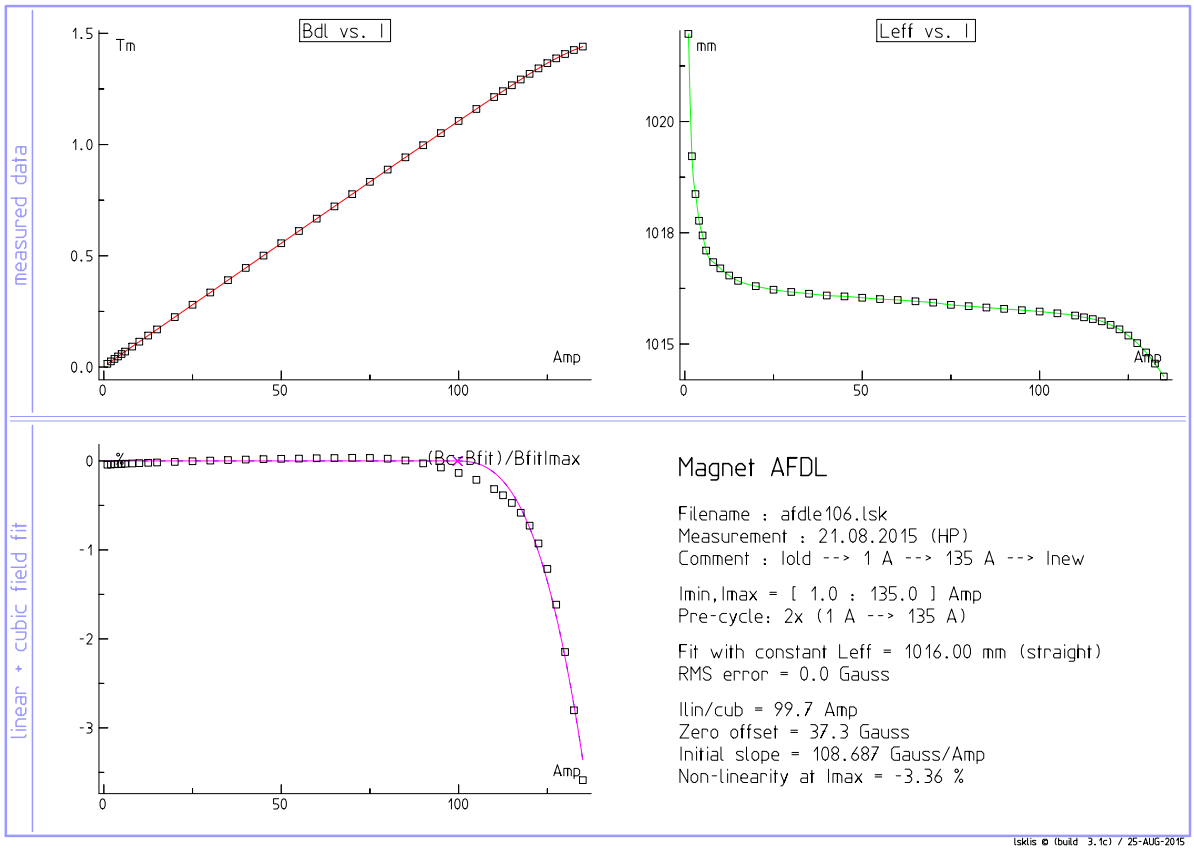

Correction coil

The magnet was demagnetized before measuring with the correction coil. Two field maps at the maximal current of +10 A and at -10 A were measured.

The power supply connected to the correction coils was our MSG2.3, 24 V / 10 A.

There is a slight difference between the fields at +10 A and the fields at -10 A. The field integrals differ between the two cases by ±1% which can be attributed to either the PS offset or to the Hall probe calibration that is never accurate at low fields. A smaller part of contribution to the difference is due to the imperfect demagnetization at the pole ends. In one case the remanent fields at the pole end add to the field and in the other they subtract from.

current [A]	B0 [Gauss]	B·dz [Tm]	Δ(B·dz) [%]
+10	-199.6	-0.02025	1.1%
-10	194.6	0.01982	-1.1%
		0.02004	

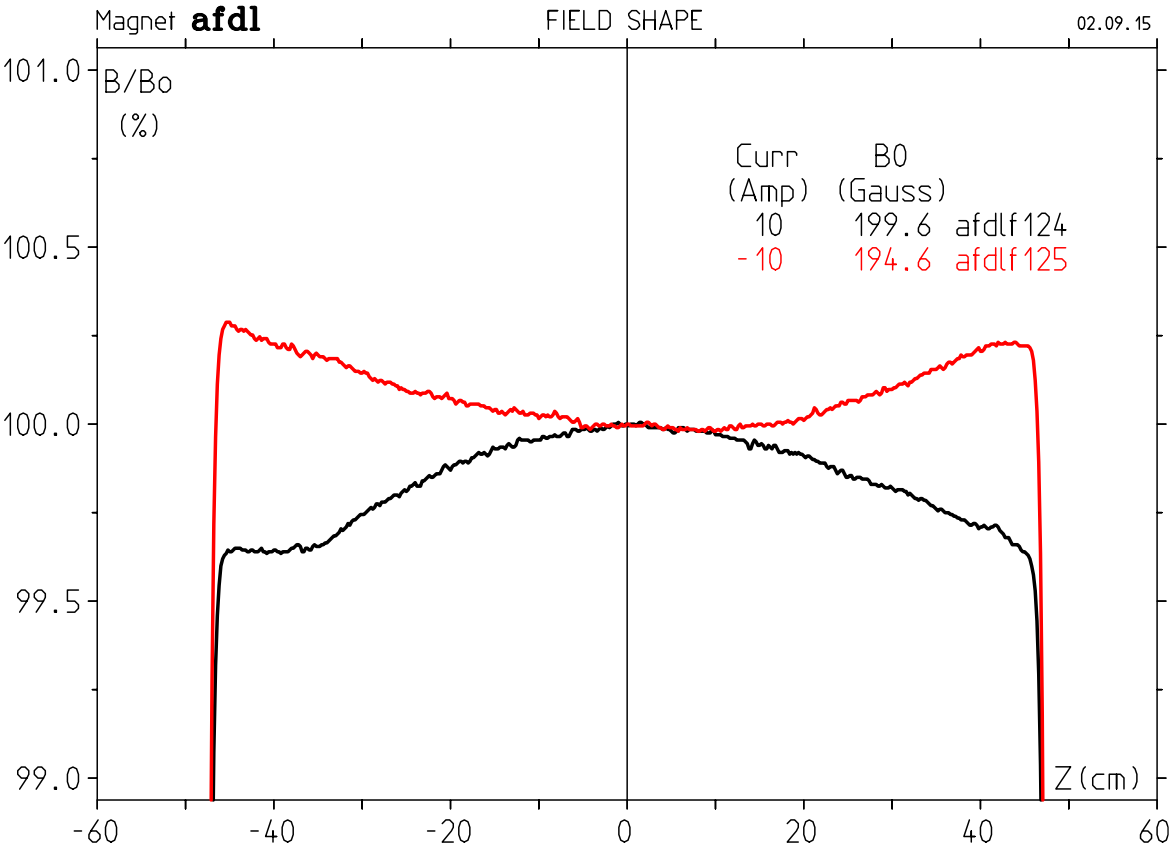

Field maps (longitudinal field profile)

The magnet was pre-cycled 2 times around the hysteresis loop with currents from 1 A to 135 A. Then the field maps were measured at various currents. Each current was set directly from 135 A with at least of 30 s waiting time.

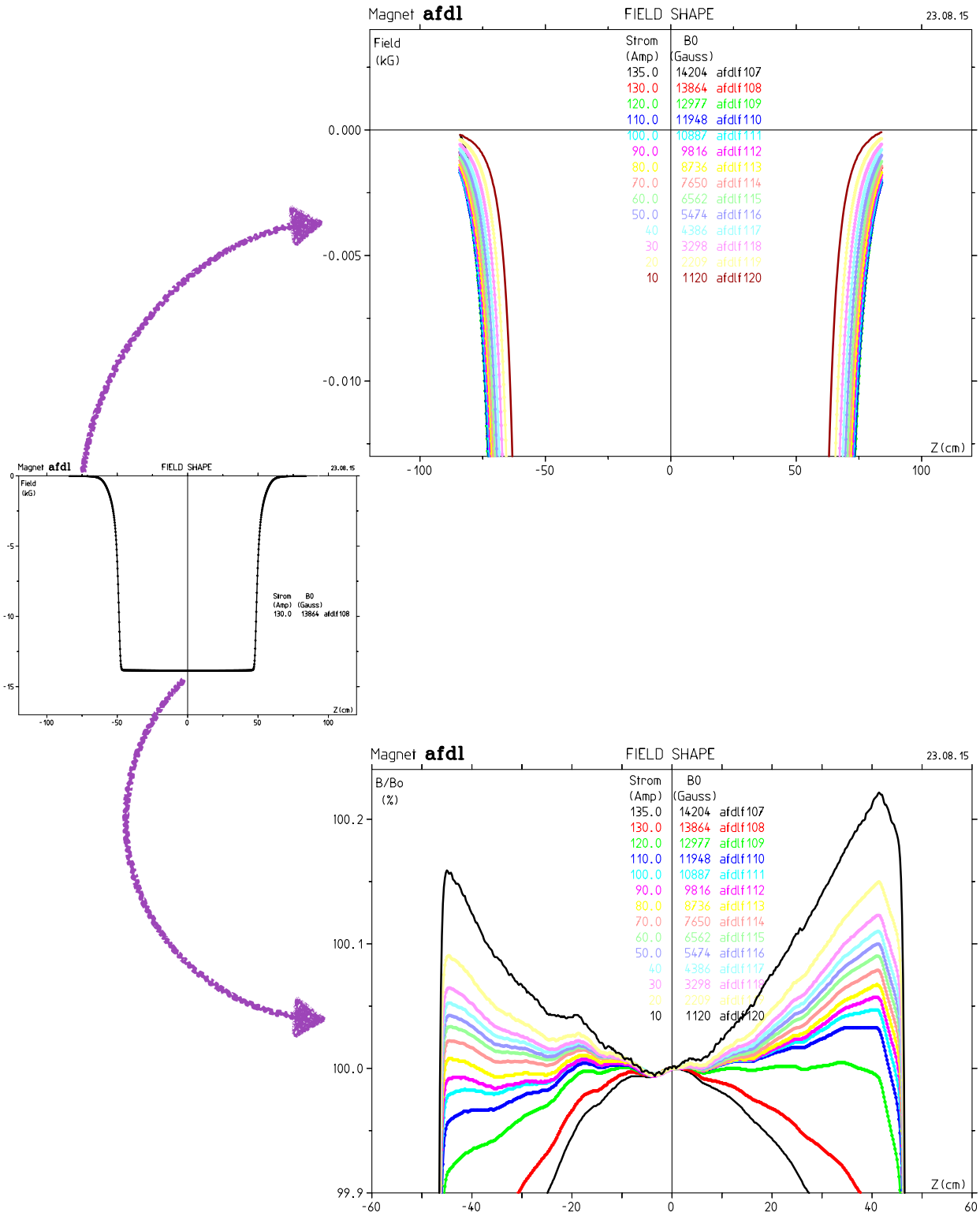

Field maps (polynomial fit on the straight field integrals)

The central region of X = ±30 mm (±5 mm over 20° bend with sagitta 44.4 mm) is analyzed with a polynomial fit up to the 4th order to the straight field integrals B·dz. B_1 represents a quadrupole component, B_2 is sextupole and B_3 is octupole component.

Only sextupole component is evident at -33±1 ppm at 5 mm distance from the central line, the other components are negligible. The small quadrupole component is a sign of a constant pole gap.

hysteresis loop +1 A → +135 A; X = -130 : +70, Y = 0, Z = -840 : +840 (23–26 August 2015)							
I A	**in** **out**	**B·dz** Tm	**B_0** Gauss	**L_{EFF}** mm	**B_1/B_0** ppm/cm	**B_2/B_0** ppm/cm^2	**B_3/B_0** ppm/cm^3
135	f 107	-1.44065	-14203.8	1014.3	9	-146	0
130	f 108	-1.40695	-13863.9	1014.8	6	-139	0
120	f 109	-1.31776	-12977.2	1015.4	6	-133	0
110	f 110	-1.21353	-11948.3	1015.7	7	-134	1
100	f 111	-1.10584	-10887.0	1015.7	11	-131	0
90	f 112	-0.99705	-9815.5	1015.8	5	-130	1
80	f 113	-0.88743	-8735.8	1015.9	7	-129	1
70	f 114	-0.77715	-7649.7	1015.9	5	-129	0
60	f 115	-0.66669	-6562.0	1016.0	4	-132	1
50	f 116	-0.55618	-5474.0	1016.0	8	-131	0
40	f 117	-0.44566	-4386.0	1016.1	6	-132	0
30	f 118	-0.33510	-3297.7	1016.2	3	-133	1
20	f 119	-0.22449	-2208.9	1016.3	1	-135	1
10	f 120	-0.11384	-1119.7	1016.7	-6	-140	2
1	f 121	-0.01420	-138.9	1022.1	8	-223	-1
0	f 122	-0.00323	-30.8				
dg	f 123	0.00001	-0.3				

Field integral homogeneity, beam vertex (*TRACK*)

Fit *Bdl(x)* with the function:

$$Bdl_{fit}(x) = Bdl_0 \cdot (1 + a_1 \cdot x + a_2 \cdot x^2 + \ldots)$$

where *x* is a distance transversal to the beam direction.

The vertex point distance to the magnet center is free to choose. Distances from 67 mm to 74 mm (the maximum possible considering the vacuum chamber position in respect to the magnet return yoke - Adriano Zandonella) were investigated.

The field inhomogeneity coming from a_1 (quadrupole) at 5 mm from the beam centre is 278±3 ppm over the whole magnet excitation range (20-130 A). The field integral on the inner side of the beam bend is weaker, the outer side is stronger. The maximal field inhomogeneity from the sextupole component a_2 is -40±3 ppm.

afdl.set in TRACK
copy & paste look.set in TRACK
quadFit.py `cat track.out`

TRACK	E MeV	$X_{Z=+1000}$ mm	V_X mm	V_Z mm	beam offset mm	Bdl_0 Tm	a_1 ppm/cm	a_2 ppm/cm^2
1 A	11.74	-109.333	67.0	-0.0	-0.0	-0.01425	241	-205
10 A	97.66	-109.369	67.0	-0.1	-0.0	-0.11431	537	-173
20 A	193.09	-109.371	67.0	-0.1	-0.0	-0.22543	548	-179
30 A	288.48	-109.373	67.0	-0.1	-0.0	-0.33650	549	-157
40 A	383.83	-109.374	67.0	-0.1	-0.0	-0.44752	552	-166
50 A	479.15	-109.374	67.0	-0.1	-0.0	-0.55850	558	-160
60 A	574.45	-109.374	67.0	-0.1	-0.0	-0.66947	556	-177
70 A	669.73	-109.374	67.0	-0.1	-0.0	-0.78041	565	-148
80 A	764.82	-109.374	67.0	-0.1	-0.0	-0.89114	562	-158
90 A	859.36	-109.373	67.0	-0.1	-0.0	-1.00121	563	-158
100 A	953.18	-109.373	67.0	-0.1	-0.0	-1.11045	563	-164
110 A	1046.04	-109.372	67.0	-0.1	-0.0	-1.21858	544	-142
120 A	1135.94	-109.374	67.0	-0.1	-0.0	-1.32326	559	-145
130 A	1212.85	-109.379	67.0	-0.1	-0.1	-1.41281	559	-173
135 A	1241.89	-109.382	67.0	-0.2	-0.1	-1.44662	549	-165
			67.0	**-0.1**	**-0.0**		**557**	**-161**

Field integral homogeneity, beam vertex (*TRACK*)

On the other hand if the distance between the magnet center and the vertex point is 74 mm, the quadrupole component at 5 mm from the beam centre decreases from 278±3 ppm to 90±5 ppm but the sextupole component gets bigger from -40±3 ppm to -103±2 ppm.

afdl.set in TRACK **copy & paste look.set in TRACK** **quadFit.py `cat track.out`**								
TRACK	**E** MeV	**$X_{Z=+1000}$** mm	**V_X** mm	**V_Z** mm	**beam offset** mm	**Bdl_0** Tm	**a_1** ppm/cm	**a_2** ppm/cm^2
1 A	11.74	-109.340	74.0	-0.0	-0.0	-0.01425	-164	-428
10 A	97.69	-109.370	74.0	-0.1	-0.0	-0.11434	146	-428
20 A	193.15	-109.372	74.0	-0.1	-0.0	-0.22549	167	-425
30 A	288.56	-109.373	74.0	-0.1	-0.0	-0.33659	170	-408
40 A	383.94	-109.375	74.0	-0.1	-0.0	-0.44765	177	-407
50 A	479.29	-109.375	74.0	-0.1	-0.0	-0.55866	186	-407
60 A	574.61	-109.375	74.0	-0.1	-0.0	-0.66966	181	-416
70 A	669.93	-109.375	74.0	-0.1	-0.0	-0.78064	190	-405
80 A	765.05	-109.375	74.0	-0.1	-0.0	-0.89140	190	-412
90 A	859.61	-109.373	74.0	-0.1	-0.0	-1.00150	187	-417
100 A	953.45	-109.373	74.0	-0.1	-0.0	-1.11077	189	-405
110 A	1046.34	-109.373	74.0	-0.1	-0.0	-1.21893	182	-417
120 A	1136.27	-109.375	74.0	-0.1	-0.0	-1.32364	181	-426
130 A	1213.19	-109.380	74.0	-0.2	-0.1	-1.41320	164	-404
135 A	1242.23	-109.383	74.0	-0.2	-0.1	-1.44702	150	-420
			74.0	**-0.1**	**-0.0**		**180**	**-412**

Beam vertex point

The beam vertex position is insensitive to the magnet excitation to ±0.1 mm.

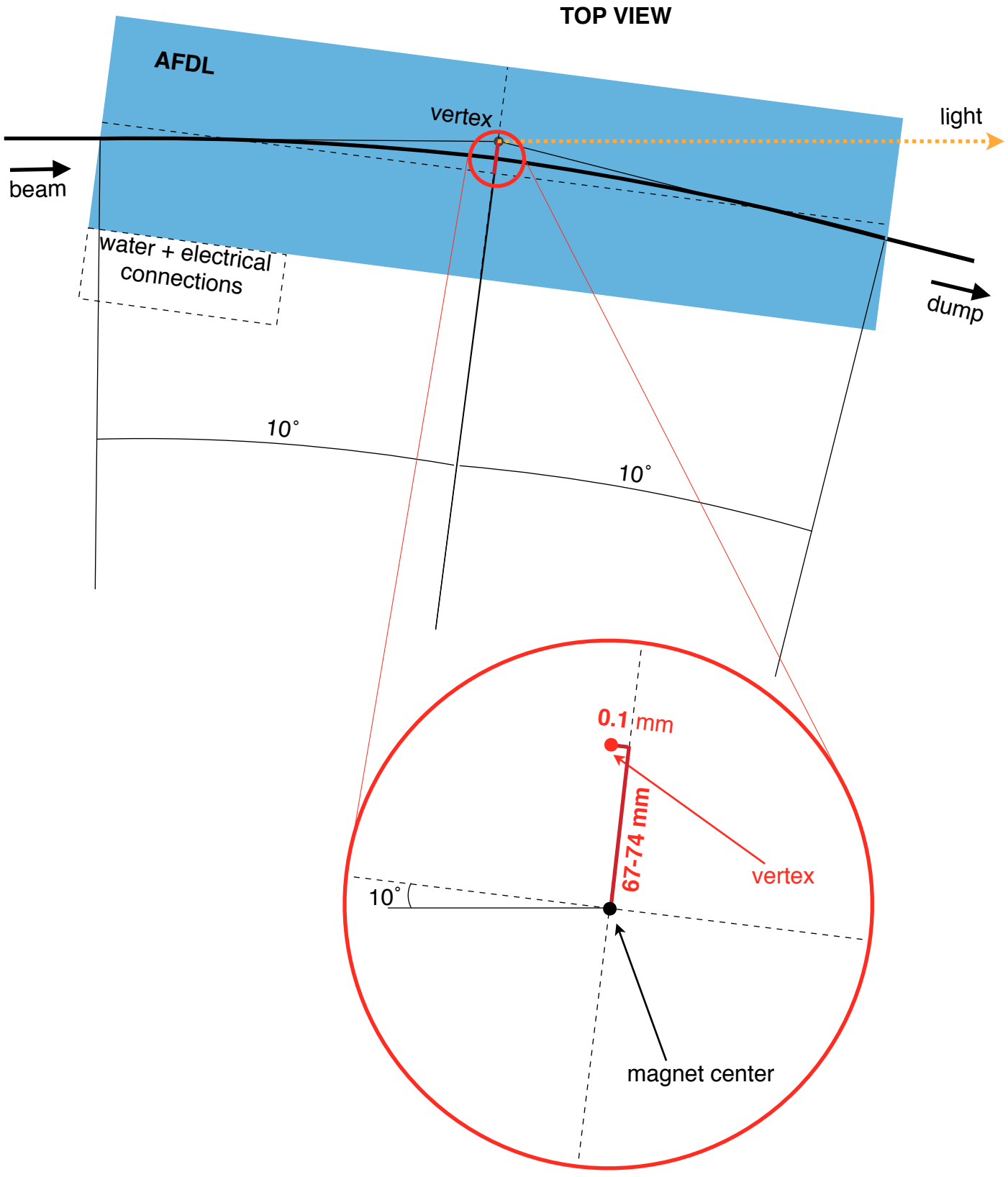

Magnet AFDL

File : afdle106.lsk
Date : 21.08.2015
Meas-type : HP
Comment : Iold --> 1 A --> 135 A --> Inew

Pre-cycle : 2x (1 A --> 135 A)

#Curr: 39 (nPaths=1)
Z-dir: from -840.00 to 840.00 mm, steps of 2.00 mm
X-dir: at 0.000 mm

linear_<1:Ilin> and cubic_<Ilin:Imax> approximation of Bc:
Blin = b0 + b1 * Irel ; Irel = I / Imax
Bcub = Blin + b2 * Irel^2 + b3 * Irel^3 ; Irel = (I - Ilin) / (Imax - Ilin)

	Ilin_A	Imax_A	b0_G	b1_G	b2_G	b3_G	RMS_G
\	99.7	135.0	37.3	14670.1	-115.9	-378.1	11.1

\ = decreasing current branch

constLeff (straight) = 1016.00 mm
constLeff = 1021.2 mm
constBendingRadius = 2925.5 mm
fullBendingAngle = 20.0 deg
Leff / Lz = 1.00510
particle E0 = 0.511 MeV

I_Amp	Bdz_Gmm	p_MeV/c	E_MeV	Bc_G	err_G
134.98*	14406638.0	1242.438	1241.927	14179.8	-33.6
132.48\	14247812.0	1228.741	1228.230	14023.4	-8.8
129.98\	14069789.0	1213.388	1212.877	13848.2	8.7
127.48\	13873462.0	1196.457	1195.946	13655.0	19.1
124.98\	13657282.0	1177.813	1177.302	13442.2	20.3
122.48\	13423873.0	1157.684	1157.173	13212.5	13.8
119.98\	13177808.0	1136.463	1135.952	12970.3	3.3
117.48\	12923504.0	1114.531	1114.021	12720.0	-7.7
114.98\	12663857.0	1092.139	1091.629	12464.4	-16.9
112.48\	12400824.0	1069.455	1068.944	12205.5	-23.5
109.98\	12135125.0	1046.541	1046.030	11944.0	-27.3
104.98\	11598754.0	1000.284	999.773	11416.1	-27.3
99.98\	11058612.0	953.702	953.191	10884.5	-19.8
94.98\	10515378.0	906.853	906.342	10349.8	-10.8
89.99\	9970590.0	859.870	859.359	9813.6	-4.0
84.99\	9423407.0	812.681	812.170	9275.0	0.7
79.99\	8874386.0	765.333	764.822	8734.6	3.7
74.99\	8323782.0	717.848	717.338	8192.7	5.0
69.99\	7771794.5	670.245	669.734	7649.4	5.2
64.99\	7219446.0	622.610	622.099	7105.8	4.8
59.99\	6666903.5	574.958	574.447	6561.9	4.4
54.99\	6114463.5	527.315	526.805	6018.2	3.8
49.99\	5561911.0	479.663	479.152	5474.3	3.4
44.99\	5009328.5	432.008	431.497	4930.4	2.9
40.00\	4456683.0	384.347	383.837	4386.5	2.1
35.00\	3903959.5	336.680	336.169	3842.5	1.5
30.00\	3351045.8	288.996	288.486	3298.3	0.6
25.00\	2797991.3	241.301	240.790	2753.9	-0.4
20.00\	2244919.0	193.603	193.093	2209.6	-1.6
15.00\	1691697.1	145.893	145.383	1665.1	-2.6
12.50\	1415221.3	122.050	121.540	1392.9	-3.2
10.00\	1138477.6	98.183	97.673	1120.5	-3.7
8.00\	917186.4	79.099	78.589	902.7	-4.2
6.00\	695902.9	60.015	59.506	684.9	-4.6
5.00\	585219.4	50.470	49.961	576.0	-5.1
4.00\	474584.6	40.928	40.421	467.1	-5.2
3.00\	363865.3	31.380	30.873	358.1	-5.5
2.00\	253071.1	21.825	21.320	249.1	-5.8
1.00*	142105.6	12.255	11.755	139.9	-6.2

p = Bdz / fullBendingAngle * Leff / Lz * c * e-13 * factor
factor = p(TRACK) / p(LSKLIS) = 0.99906
E = sqrt(E0^2 + p^2) - E0
Bc = Bdz / constLeff
err = Bc - Bfit

I [A]	p(lsklis) factor = 1	p(TRACK) vx = 67 mm	factor	error
1	12.27	12.24	0.99787	-0.119%
10	98.28	98.17	0.99893	-0.013%
20	193.79	193.60	0.99906	0.001%
30	289.27	288.99	0.99905	-0.001%
40	384.71	384.34	0.99905	-0.001%
50	480.11	479.66	0.99905	-0.000%
60	575.50	574.96	0.99907	0.001%
70	670.88	670.24	0.99905	-0.000%
80	766.05	765.34	0.99906	0.001%
90	860.68	859.87	0.99907	0.001%
100	954.60	953.69	0.99905	-0.001%
110	1047.53	1046.55	0.99907	0.002%
120	1137.53	1136.45	0.99905	-0.000%
130	1214.53	1213.36	0.99904	-0.002%
135	1243.61	1242.41	0.99903	-0.002%
			0.99906	

Magnet AFDL

File : afdle106.lsk
Date : 21.08.2015
Meas-type : HP
Comment : Iold --> 1 A --> 135 A --> Inew

Pre-cycle : 2x (1 A --> 135 A)

#Curr: 39 (nPaths=1)
Z-dir: from -840.00 to 840.00 mm, steps of 2.00 mm
X-dir: at 0.000 mm

linear_<1:Ilin> and cubic_<Ilin:Imax> approximation of Bc:
Blin = b0 + b1 * Irel ; Irel = I / Imax
Bcub = Blin + b2 * Irel^2 + b3 * Irel^3 ; Irel = (I - Ilin) / (Imax - Ilin)

	Ilin_A	Imax_A	b0_G	b1_G	b2_G	b3_G	RMS_G
\	99.7	135.0	37.3	14670.1	-115.9	-378.1	11.1

\ = decreasing current branch

constLeff (straight) = 1016.00 mm
constLeff = 1021.2 mm
constBendingRadius = 2925.5 mm
fullBendingAngle = 20.0 deg
Leff / Lz = 1.00510
particle E0 = 0.511 MeV

I_Amp	Bdz_Gmm	p_MeV/c	E_MeV	Bc_G	err_G
134.98*	14406638.0	1242.786	1242.275	14179.8	-33.6
132.48\	14247812.0	1229.085	1228.574	14023.4	-8.8
129.98\	14069789.0	1213.728	1213.217	13848.2	8.7
127.48\	13873462.0	1196.792	1196.281	13655.0	19.1
124.98\	13657282.0	1178.143	1177.632	13442.2	20.3
122.48\	13423873.0	1158.008	1157.497	13212.5	13.8
119.98\	13177808.0	1136.781	1136.271	12970.3	3.3
117.48\	12923504.0	1114.844	1114.333	12720.0	-7.7
114.98\	12663857.0	1092.446	1091.935	12464.4	-16.9
112.48\	12400824.0	1069.755	1069.244	12205.5	-23.5
109.98\	12135125.0	1046.834	1046.323	11944.0	-27.3
104.98\	11598754.0	1000.564	1000.054	11416.1	-27.3
99.98\	11058612.0	953.969	953.458	10884.5	-19.8
94.98\	10515378.0	907.107	906.596	10349.8	-10.8
89.99\	9970590.0	860.111	859.600	9813.6	-4.0
84.99\	9423407.0	812.909	812.398	9275.0	0.7
79.99\	8874386.0	765.547	765.037	8734.6	3.7
74.99\	8323782.0	718.050	717.539	8192.7	5.0
69.99\	7771794.5	670.433	669.922	7649.4	5.2
64.99\	7219446.0	622.784	622.273	7105.8	4.8
59.99\	6666903.5	575.119	574.608	6561.9	4.4
54.99\	6114463.5	527.463	526.952	6018.2	3.8
49.99\	5561911.0	479.797	479.287	5474.3	3.4
44.99\	5009328.5	432.129	431.618	4930.4	2.9
40.00\	4456683.0	384.455	383.944	4386.5	2.1
35.00\	3903959.5	336.774	336.264	3842.5	1.5
30.00\	3351045.8	289.077	288.567	3298.3	0.6
25.00\	2797991.3	241.368	240.858	2753.9	-0.4
20.00\	2244919.0	193.658	193.147	2209.6	-1.6
15.00\	1691697.1	145.934	145.424	1665.1	-2.6
12.50\	1415221.3	122.084	121.574	1392.9	-3.2
10.00\	1138477.6	98.211	97.701	1120.5	-3.7
8.00\	917186.4	79.121	78.612	902.7	-4.2
6.00\	695902.9	60.032	59.523	684.9	-4.6
5.00\	585219.4	50.484	49.975	576.0	-5.1
4.00\	474584.6	40.940	40.432	467.1	-5.2
3.00\	363865.3	31.389	30.882	358.1	-5.5
2.00\	253071.1	21.831	21.326	249.1	-5.8
1.00*	142105.6	12.259	11.758	139.9	-6.2

p = Bdz / fullBendingAngle * Leff / Lz * c * e-13 * factor
factor = p(TRACK) / p(LSKLIS) = 0.99934
E = sqrt(E0^2 + p^2) - E0
Bc = Bdz / constLeff
err = Bc - Bfit

I [A]	p(lsklis) factor = 1	p(TRACK) vx = 74 mm	factor	error
1	12.27	12.24	0.99792	-0.142%
10	98.28	98.20	0.99919	-0.015%
20	193.79	193.66	0.99934	-0.000%
30	289.27	289.07	0.99933	-0.001%
40	384.71	384.45	0.99933	-0.001%
50	480.11	479.80	0.99934	-0.000%
60	575.50	575.12	0.99935	0.001%
70	670.88	670.44	0.99935	0.001%
80	766.05	765.56	0.99935	0.001%
90	860.68	860.12	0.99935	0.001%
100	954.60	953.96	0.99934	-0.000%
110	1047.53	1046.85	0.99935	0.002%
120	1137.53	1136.78	0.99934	0.000%
130	1214.53	1213.70	0.99932	-0.002%
135	1243.61	1242.74	0.99931	-0.003%
			0.99934	

Lookup table: magnet current ↔ beam energy (vertex position vx = 67 mm)

I	Energy	I	Energy	I	Energy	I	Energy	I	Energy
-2 A	21.30 MeV	-29 A	278.97 MeV	-56 A	536.40 MeV	-83 A	793.37 MeV	-110 A	1046.22 MeV
-3 A	30.85 MeV	-30 A	288.51 MeV	-57 A	545.94 MeV	-84 A	802.83 MeV	-111 A	1055.41 MeV
-4 A	40.40 MeV	-31 A	298.05 MeV	-58 A	555.47 MeV	-85 A	812.29 MeV	-112 A	1064.57 MeV
-5 A	49.93 MeV	-32 A	307.58 MeV	-59 A	565.00 MeV	-86 A	821.75 MeV	-113 A	1073.69 MeV
-6 A	59.50 MeV	-33 A	317.12 MeV	-60 A	574.53 MeV	-87 A	831.19 MeV	-114 A	1082.78 MeV
-7 A	69.05 MeV	-34 A	326.66 MeV	-61 A	584.06 MeV	-88 A	840.63 MeV	-115 A	1091.83 MeV
-8 A	78.58 MeV	-35 A	336.20 MeV	-62 A	593.59 MeV	-89 A	850.07 MeV	-116 A	1100.83 MeV
-9 A	88.12 MeV	-36 A	345.73 MeV	-63 A	603.12 MeV	-90 A	859.49 MeV	-117 A	1109.77 MeV
-10 A	97.66 MeV	-37 A	355.27 MeV	-64 A	612.65 MeV	-91 A	868.91 MeV	-118 A	1118.65 MeV
-11 A	107.21 MeV	-38 A	364.81 MeV	-65 A	622.19 MeV	-92 A	878.32 MeV	-119 A	1127.45 MeV
-12 A	116.75 MeV	-39 A	374.34 MeV	-66 A	631.72 MeV	-93 A	887.73 MeV	-120 A	1136.15 MeV
-13 A	126.29 MeV	-40 A	383.88 MeV	-67 A	641.25 MeV	-94 A	897.12 MeV	-121 A	1144.74 MeV
-14 A	135.84 MeV	-41 A	393.41 MeV	-68 A	650.78 MeV	-95 A	906.51 MeV	-122 A	1153.20 MeV
-15 A	145.38 MeV	-42 A	402.95 MeV	-69 A	660.31 MeV	-96 A	915.89 MeV	-123 A	1161.49 MeV
-16 A	154.93 MeV	-43 A	412.48 MeV	-70 A	669.84 MeV	-97 A	925.27 MeV	-124 A	1169.59 MeV
-17 A	164.47 MeV	-44 A	422.02 MeV	-71 A	679.36 MeV	-98 A	934.63 MeV	-125 A	1177.48 MeV
-18 A	174.00 MeV	-45 A	431.55 MeV	-72 A	688.89 MeV	-99 A	943.99 MeV	-126 A	1185.13 MeV
-19 A	183.54 MeV	-46 A	441.09 MeV	-73 A	698.40 MeV	-100 A	953.34 MeV	-127 A	1192.51 MeV
-20 A	193.08 MeV	-47 A	450.62 MeV	-74 A	707.92 MeV	-101 A	962.68 MeV	-128 A	1199.62 MeV
-21 A	202.63 MeV	-48 A	460.16 MeV	-75 A	717.43 MeV	-102 A	972.02 MeV	-129 A	1206.45 MeV
-22 A	212.17 MeV	-49 A	469.69 MeV	-76 A	726.94 MeV	-103 A	981.34 MeV	-130 A	1213.03 MeV
-23 A	221.71 MeV	-50 A	479.22 MeV	-77 A	736.45 MeV	-104 A	990.66 MeV	-131 A	1219.38 MeV
-24 A	231.26 MeV	-51 A	488.75 MeV	-78 A	745.95 MeV	-105 A	999.96 MeV	-132 A	1225.45 MeV
-25 A	240.80 MeV	-52 A	498.28 MeV	-79 A	755.45 MeV	-106 A	1009.25 MeV	-133 A	1231.21 MeV
-26 A	250.34 MeV	-53 A	507.81 MeV	-80 A	764.94 MeV	-107 A	1018.52 MeV	-134 A	1236.70 MeV
-27 A	259.88 MeV	-54 A	517.34 MeV	-81 A	774.42 MeV	-108 A	1027.78 MeV		
-28 A	269.43 MeV	-55 A	526.87 MeV	-82 A	783.90 MeV	-109 A	1037.01 MeV		

Lookup table: magnet current ↔ beam energy (vertex position vx = 74 mm)

I	Energy	I	Energy	I	Energy	I	Energy	I	Energy
-2 A	21.31 MeV	-29 A	279.04 MeV	-56 A	536.55 MeV	-83 A	793.59 MeV	-110 A	1046.52 MeV
-3 A	30.86 MeV	-30 A	288.59 MeV	-57 A	546.09 MeV	-84 A	803.06 MeV	-111 A	1055.71 MeV
-4 A	40.41 MeV	-31 A	298.13 MeV	-58 A	555.63 MeV	-85 A	812.52 MeV	-112 A	1064.87 MeV
-5 A	49.95 MeV	-32 A	307.67 MeV	-59 A	565.16 MeV	-86 A	821.98 MeV	-113 A	1074.00 MeV
-6 A	59.51 MeV	-33 A	317.21 MeV	-60 A	574.69 MeV	-87 A	831.43 MeV	-114 A	1083.09 MeV
-7 A	69.07 MeV	-34 A	326.75 MeV	-61 A	584.23 MeV	-88 A	840.87 MeV	-115 A	1092.13 MeV
-8 A	78.60 MeV	-35 A	336.29 MeV	-62 A	593.76 MeV	-89 A	850.30 MeV	-116 A	1101.13 MeV
-9 A	88.15 MeV	-36 A	345.83 MeV	-63 A	603.29 MeV	-90 A	859.73 MeV	-117 A	1110.08 MeV
-10 A	97.69 MeV	-37 A	355.37 MeV	-64 A	612.83 MeV	-91 A	869.15 MeV	-118 A	1118.96 MeV
-11 A	107.24 MeV	-38 A	364.91 MeV	-65 A	622.36 MeV	-92 A	878.57 MeV	-119 A	1127.76 MeV
-12 A	116.78 MeV	-39 A	374.45 MeV	-66 A	631.89 MeV	-93 A	887.98 MeV	-120 A	1136.47 MeV
-13 A	126.33 MeV	-40 A	383.98 MeV	-67 A	641.43 MeV	-94 A	897.37 MeV	-121 A	1145.06 MeV
-14 A	135.88 MeV	-41 A	393.52 MeV	-68 A	650.96 MeV	-95 A	906.77 MeV	-122 A	1153.52 MeV
-15 A	145.42 MeV	-42 A	403.06 MeV	-69 A	660.50 MeV	-96 A	916.15 MeV	-123 A	1161.81 MeV
-16 A	154.97 MeV	-43 A	412.60 MeV	-70 A	670.03 MeV	-97 A	925.53 MeV	-124 A	1169.92 MeV
-17 A	164.51 MeV	-44 A	422.14 MeV	-71 A	679.55 MeV	-98 A	934.89 MeV	-125 A	1177.81 MeV
-18 A	174.05 MeV	-45 A	431.68 MeV	-72 A	689.08 MeV	-99 A	944.26 MeV	-126 A	1185.46 MeV
-19 A	183.60 MeV	-46 A	441.21 MeV	-73 A	698.60 MeV	-100 A	953.61 MeV	-127 A	1192.85 MeV
-20 A	193.14 MeV	-47 A	450.75 MeV	-74 A	708.12 MeV	-101 A	962.95 MeV	-128 A	1199.96 MeV
-21 A	202.68 MeV	-48 A	460.29 MeV	-75 A	717.63 MeV	-102 A	972.29 MeV	-129 A	1206.79 MeV
-22 A	212.23 MeV	-49 A	469.82 MeV	-76 A	727.15 MeV	-103 A	981.62 MeV	-130 A	1213.37 MeV
-23 A	221.77 MeV	-50 A	479.35 MeV	-77 A	736.66 MeV	-104 A	990.94 MeV	-131 A	1219.72 MeV
-24 A	231.32 MeV	-51 A	488.89 MeV	-78 A	746.16 MeV	-105 A	1000.24 MeV	-132 A	1225.80 MeV
-25 A	240.87 MeV	-52 A	498.42 MeV	-79 A	755.66 MeV	-106 A	1009.53 MeV	-133 A	1231.56 MeV
-26 A	250.41 MeV	-53 A	507.95 MeV	-80 A	765.15 MeV	-107 A	1018.81 MeV	-134 A	1237.05 MeV
-27 A	259.96 MeV	-54 A	517.49 MeV	-81 A	774.64 MeV	-108 A	1028.06 MeV		
-28 A	269.50 MeV	-55 A	527.02 MeV	-82 A	784.12 MeV	-109 A	1037.30 MeV		

WHBM – beam entrance magnet end

beam in	date	I A	X mm	Y mm	Z mm	comment
e 01	5 Aug 2015	29x	0	0	-1000, +100	2x ±135 A precycle, 5 A/s, 30 s waiting
f 02	6 Aug 2015	129.98	-130, +70	0	-1000, +100	2x ±135 A precycle, → 135 A → 130 A
f 03		-129.97				→ -135 A → -130 A
f 04		129.98				→ 135 A → 130 A
f 05	7 Aug 2015	-129.97				→ -135 A → -130 A
f 06		-119.97				→ -130 A → -120 A
f 07		-109.97				→ -120 A → -110 A
f 08		-99.98				→ -110 A → -100 A
f 09		-89.98				→ -100 A → -90 A
f 10_o		-49.99				→ -90 A → -50 A
f 11_o		-19.99				→ -50 A → -20 A
f 12		119.98				→ 135 A → 120 A
f 13		109.98				→ 120 A → 110 A
f 14	8 Aug 2015	99.98				→ 110 A → 100 A
f 15		89.99				→ 100 A → 90 A
f 16_o		49.99				→ 90 A → 50 A
f 17_o		20.00				→ 50 A → 20 A
l 18	10 Aug 2015	0	0	0	-670, +670	→ -135 A → +26 A → 0
l 19		0				→ 135 A → -26 A → 0
f 20		0	-130, +70	0	-1000, +100	degaussed magnet as of l 19
f 21		-79.98				→ -90 A → -80 A
f 22		-69.99				→ -80 A → -70 A
f 23		-59.99				→ -70 A → -60 A
f 24		-39.99				→ -50 A → -40 A
f 25	11 Aug 2015	-29.99				→ -40 A → -30 A
f 26		79.99				→ 90 A → 80 A
f 27		69.99				→ 80 A → 70 A
f 28		59.99				→ 70 A → 60 A
f 29		40.00				→ 50 A → 40 A
f 30		30.00				→ 40 A → 30 A

WHBM – beam entrance magnet end

beam in	date	I A	X mm	Y mm	Z mm	comment
f 10	11 Aug 2015	-49.99	-130, +70	0	-1000, +100	→ -60 A → -50 A
f 31				5		
f 32	12 Aug 2015			3.5		
f 33				-3.5		
f 34				5		
f 16		49.99	-130, +70	0	-1000, +100	→ 60 A → 50 A
f 35				5		
f 36				3.5		
f 37				-3.5		
f 38				-5		
f 17		20.00	-130, +70	0	-1000, +100	→ 30 A → 20 A
f 39		-129.97	-130, +70	0	-1000, +100	→ -135 A → -130 A
f 40_o				5		
f 41				3.5		
f 42				-3.5		
f 44	13 Aug 2015	129.98	-130, +70	0	-1000, +100	→ 135 A → 130 A
f 45				5		
f 46				3.5		
f 47				-3.5		
f 48				-5		
f 43	14 Aug 2015	-129.97	-130, +70	-5	-1000, +100	→ -135 A → -130 A
f 40				5		
f 11		-19.99	-130, +70	0	-1000, +100	→ -30 A → -20 A

WHBM – beam exit magnet end

beam out	date	I A	X mm	Y mm	Z mm	comment
l 49	15 Aug 2015	79.99	0	0	-100, +680	test line, air fan OFF
l 50						test line, air fan ON
e 51	16 Aug 2015	29x	0	0	-100, +860	2x ±135 A precycle, 5 A/s, 30 s waiting
f 52		-129.97	-130, +70	0	-100, +860	→ -135 A → -130 A
f 53		-119.97				→ -130 A → -120 A
f 54		-109.98				→ -120 A → -110 A
f 55		-99.98				→ -110 A → -100 A
f 56		-89.98				→ -100 A → -90 A
f 57		-79.98				→ -90 A → -80 A
f 58	17 Aug 2015	-69.99				→ -80 A → -70 A
f 59		-59.99				→ -70 A → -60 A
f 60		-49.99				→ -60 A → -50 A
f 61		-39.99				→ -50 A → -40 A
f 62		-29.99				→ -40 A → -30 A
f 63		-19.99				→ -30 A → -20 A
f 64		129.98				→ 135 A → 130 A
f 65		119.98				→ 130 A → 120 A
f 66		109.98				→ 120 A → 110 A
f 67		99.98				→ 110 A → 100 A
f 68		89.99				→ 100 A → 90 A
f 69		79.99				→ 90 A → 80 A
f 70		69.99				→ 80 A → 70 A
f 71	18 Aug 2015	59.99				→ 70 A → 60 A
f 72		49.99				→ 60 A → 50 A
f 73		40.00				→ 50 A → 40 A
f 74		30.00				→ 40 A → 30 A
f 75		20.00				→ 30 A → 20 A

Coil - water cooling

I = 135 A (4 bar, 6.1 l/min)							
time	**Δt**	**T_{IN}**	**T_{OUT}**	**ΔT_{water}**		**U_{tot}**	**ΔT_{av_coil}**
13:00		30.0	29.9	-0.1		**30.20**	
13:05	5m	30.0	36.9	6.9	75%	30.82	4.7
13:10	10m	30.0	38.7	8.7	95%	30.97	5.9
13:15	15m	30.0	39.0	9.0	98%	30.99	6.0
13:20	20m	30.0	39.1	9.1	99%	31.00	6.1
13:30	30m	30.0	39.1	9.1	99%	31.00	6.1
14:12	1h 12m	30.0	39.2	9.2	100%	31.00	6.1
14:55	1h 55m	30.0	39.2	9.2	100%	31.01	6.2
16:00	3h	30.0	39.2	**9.2**	100%	**31.01**	6.2

I = 50 A then 130 A (4 bar, 6.0 l/min)							
time	**Δt**	**T_{IN}**	**T_{OUT}**	**ΔT_{water}**		**U_{tot}**	**ΔT_{av_coil}**
18:40		30.0	30.1	0.1		**11.17**	
18:45	5m	30.0	30.8	0.8	67%	11.20	0.6
18:50	10m	30.0	31.2	1.2	100%	11.20	0.6
19:00	20m	30.0	31.2	**1.2**	100%	**11.21**	0.8
19:00		30.0	31.6	1.6	19%	**29.18**	
19:05	5m	30.0	35.9	5.9	69%	29.61	3.4
19:10	10m	30.0	37.9	7.9	92%	29.75	4.5
19:20	20m	30.0	38.5	8.5	99%	29.79	4.8
20:00	1h	30.0	38.6	**8.6**	100%	**29.80**	4.9